Geochemical Perspectives Letters

Calcium stable isotopes place Devonian conodonts as first level consumers

V. Balter, J.E. Martin, T. Tacail, G. Suan, S. Renaud, C. Girard

Supplementary Information

The Supplementary Information includes:

- Supplementary Material
- Supplementary Method
- Supplementary Discussion
- Tables S-1 to S-5
- Figures S-1 to S-3
- Supplementary Information References

Supplementary Material

Conodont elements were collected from Frasnian-Famennian levels of five different localities (Figure S-1): 1) a Famennian succession at the Col des Tribes (France), a newly described outcrop in the Montagne Noire, which exposes a continuous record of the Famennian Stage (Girard *et al*. 2014); 2) the stratotype area of the F/F boundary, the Coumiac Lower Quarry, located close to the Col des Tribes (Girard and Feist 1997); 3) M'rirt (Central Meseta, Morocco), which shows a similar environmental context to Coumiac, where deposits are a succession of well-oxygenated beds (Lazreq 1999). Conodonts are sampled from the *Pa. linguiformis* Zone (M9, level just before the Upper Kellwasser event) (Girard *et al.* 2005); 4) the Xom Nha section (Central Vietnam), which is characterised by a continuous carbonate sequence dated from latest Frasnian to Famennian (here the conodonts are from the *Pa. linguiformis* Zone XN52, Phuong 1998); 5) Sprite Ridge (Canning Basin, Australia), which is part of an elongated Famennian limestone (Feist and Becker 1997). The sample analysed here is of the *Early rhomboidea* Zone. In addition, a brachiopod sample was collected from the La Serre section in the *Bispathodus ultimus* zone corresponding to the CT69 level at Col des Tribes. All correlations are based on conodont biostratigraphy (Flajs and Feist 1988; Girard and Feist 1997; Girard *et al.* 2010, 2014), and absolute ages are given in Figure S-1 according to Becker *et al*. (2012). All the samples came from stratigraphic levels around the F/F boundary which is dated of ~ 372 Ma. Calcium isotopes were measured in a total of 80 conodont samples, which are distributed as follows: *Palmatolepis,* n = 38; *Ancyrodella,* n = 12; *Ancyrognathus,* n = 11; *Icriodus* n = 5; *Polygnathus,* n = 14. For each studied stratigraphic level and for a given genus, between five and twenty conodont elements (depending on their size and the richness of the stratigraphic layer) were selected and completely dissolved in 1 ml ultrapure concentrated HNO_3 overnight. The brachiopod shell was sampled following the protocol of Brazier *et al*. (2015) and dissolved as for the conodonts.

Supplementary Methods

The details of the purification processes and analytical techniques are given in Tacail *et al*. (2014) but are summarised here. Samples were digested on hotplate using 2 ml concentrated distilled HNO_3. Vials were heated at 120°C during 2 h and regularly degassed. A volume of 2 ml Suprapur 30 % H_2O_2 was added on cooled samples and vials were sealed, regularly degassed at ambient temperature. Finally, vials were sealed and heated on hotplate at 100°C during 2 h and evaporated to dryness. The use of MC-ICPMS requires efficient separation of Ca from samples because of isobaric interferences. Strontium, potassium and to a lesser extent magnesium from samples have to be eliminated to avoid any bias in the measurement of $^{42}Ca^+$ (interfering with $^{84}Sr^{2+}$, $^{41}K^1H^+$ and $^{25}Mg^{16}O^+$), $^{43}Ca^+$ ($^{86}Sr^{2+}$) and $^{44}Ca^+$ ($^{88}Sr^{2+}$, $^{26}Mg^{18}O^+$). The elimination of the remaining matrix components is also required to avoid any bias due to matrix effects. The exact elution procedure is shown in Table S-1.

The first elution aims at discarding K and the majority of matrix elements. Once taken up in 1N HCl, samples were processed on 0.76 cm internal diameter Teflon chromatography columns, filled with 2 ml of Biorad AG50W-X12 cationic resin, 200-400 mesh. The AG50W-X12 columns were reused maximum 5 times, in order to avoid any aging of resin. Strontium was finally eliminated by processing samples on 0.7 ml Eichrom Sr-specific resin, packed in 2 ml Eichrom columns, following a classical Sr elimination protocol (Table S-1). Blank levels never exceed 100 ng, which would represent a contribution of 1/30 of a typical signal. The Sr/Ca ratio, measured as the $^{87}Sr^{2+}/^{44}Ca^+$ ratio is always below 10^{-5}. Quality control of the Ca chemical purification is controlled in each session by including a blank and one or two standards which are matrix-matched with the samples (SRM915b "Calcium Carbonate" and SRM1486 "Bone Meal"). Data for the standards are reported in Table S-2. Based on replicates of two standards, the external reproducibility has been estimated at ±0.066 ‰ (2 SD, n = 130) for SRM1486 and ±0.048 ‰ (2SD, n=17) for SRM915b in the context of the present study. Since 2014, the overall reproducibility of SRM1486 is ±0.006 (2 SE, n = 404) with a mean $\delta^{44/42}Ca$ value of -1.024 ‰.

The Ca isotopic compositions were measured using a Neptune plus MC-ICPMS (Thermo Scientific, Bremen, Germany). Standard and sample solutions were prepared to reach a 3 $mg.l^{-1}$ concentration in 0.05N HNO_3 medium. Calcium solution was introduced as a dry aerosol with a Cetac Aridus II desolvating system allowing reduction of hydride and oxide formation. The Aridus desolvating system was used with Ar sweep gas flow and an additional N_2 gas flow. Aerosols were introduced in a 1200 W plasma with uptake rate of 100 to 150 $\mu L.min^{-1}$. The optimised MC-ICPMS instrument operating parameters were : cool gas (15 $L.min^{-1}$), auxiliary gas (0.7-0.8 $L.min^{-1}$) and sample gas (1-1.2 $L.min^{-1}$).

Faraday cups were set to measure $^{42}Ca^+$ signal on L4 cup, $^{43}Ca^+$ on L2 and $^{44}Ca^+$ on central cup. The use of these three isotopes is sufficient for mass-dependent stable isotopes composition measurements in biological materials. The L1 cup was used to monitor the $^{87}Sr^{2+}$ corresponding to m/z = 43.5. The 42 and 44 ion beams signals were measured with a 10^{11} Ω resistance on faraday cup and 43 signal was measured with 10^{12} Ω resistance, because of the low abundance of ^{43}Ca (0.135 % of total Ca). Calcium concentrations were adjusted to be within 10 % of the fixed 3 $mg.l^{-1}$ concentration. Medium mass resolution was sufficient to resolve polyatomic interferences: including $^{40}Ar^1H_2^+$, $^{12}C^{16}O_2^+$ and $^{14}N_3^+$.

Each analysis consisted of 40 measurements of 4.2 s integrations on m/z ratios 42, 43, 44 and 43.5. Even if Sr levels were very low due to the specific separation on the Sr-Spec resin, we corrected the double charge interferences of Sr on Ca ($^{88}Sr^{2+}$ on $^{44}Ca^+$, $^{86}Sr^{2+}$ on $^{43}Ca^+$, $^{84}Sr^{2+}$ on $^{42}Ca^+$) using the 43.5 signal corresponding to $^{87}Sr^{2+}$. The correction includes the instrumental mass bias on Sr isotopes, which was monitored using the NBS 987 standard. Corrected and uncorrected ratios were calculated for each measurement and averaged after exclusion of values higher than 1SD from average. Instrumental mass bias was corrected by standard-sample-standard bracketing. A Specpure Calcium plasma standard solution (Alfa Aesar), noted ICP-Lyon, was used as reference and bracketing in-house standard. ICP-Lyon required purification because of the presence of Sr traces responsible for significant interferences on the three measured isotopes.

Supplementary Discussion

Sedimentological analyses (Girard *et al.* 2014) at the Col des Tribes and geochemical analyses on bulk sediment ($\delta^{13}C$ and $\delta^{18}O$) at the Coumiac Quarry (Joachimski and Buggisch 1993) do not argue for any substantial post-depositional modifications. Regarding more specifically the Ca isotope composition of fossils, its use to unravel paleobiological features is in its infancy and data are still lacking to highlight potential methods to detect diagenesis of the original isotopic composition. Calcium is the major element of endogenous mineralised tissues, bone, dentine and enamel, which are made up of hydroxylapatite, and exogenous mineralised tissues, which are made up of calcite or aragonite. In both cases, Ca represents about 40 % weight of the mineral fraction, rendering Ca hardly prone to diagenesis because diagenetic fluids are incommensurably less Ca concentrated (Martin *et al.*, 2017). For instance, this led recently Pruss *et al.* (2018) to show that 600 Myr old Ediacaran shell-forming organisms had still preserved a Ca isotope signature typical of aragonite. Here, we did not measure the concentration of trace elements that specifically incorporate

hap during diagenetic processes, such as rare Earth elements (REE), due to sample size limitation. However, REE concentrations have been previously measured in conodonts at Coumiac along with the strontium/calcium ratio (Sr/Ca) and the oxygen isotope composition of phosphates ($\delta^{18}O$, Le Houedec *et al.*, 2014). From eight common layers where all the geochemical proxies have been measured, we show that, unless the strong correlation between La/Sm and La/Yb, indicative of substitution mechanisms in the context of 'extensive' or 'late' diagenesis (Reynard and Balter, 2014), no proxy is significantly correlated to any other (Table S-5).

Supplementary Tables

Table S-1 Chart of the purification processes.

1. Matrix elimination **AG50W-X12 resin (200-400 mesh) ~ 2mL**		
Step	**Eluent**	**Vol. (mL)**
Condition	1N HCl	10
Load	1N HCl	2+1
Elution (matrix)	1N HCl	55
Ca elution (Ca,Sr,Fe)	**6N HCl**	**10**
2. Sr elimination **Sr-Specific resin (Eichrom) ~ 0.7mL**		
Step	**Eluent**	**Vol. (mL)**
Condition	3N HNO3	5
Load	3N HNO3	0.5+0.5
Elution (Ca)	**3N HNO3**	**6**
Remaining on resin: Sr		

Table S-2 Ca isotope compositions of SRM1486 and SRM915b measured in the study relative to ICP-Lyon.

Standard		n	$\delta^{44/42}$ amu	2 SD	reference
SRM1486	session #				
	1	38	-0.52	0.02	
	2	29	-0.53	0.14	
	3	30	-0.50	0.07	
	4	7	-0.52	0.05	
	5	21	-0.48	0.08	
	6	5	-0.51	0.04	
	literature				
		25	-0.52	0.06	Martin *et al.* (2015)
		17	-0.48	0.07	Tacail *et al.* (2014)
		142	-0.51	0.07	Heuser and Eisenhauer (2008)*
		2	-0.50	0.07	Heuser *et al.* (2011)*
SRM915b	session #				
	1	3	-0.11	0.03	
	2	3	-0.06	0.02	
	3	3	-0.06	0.09	
	4	2	-0.06	0.05	
	5	6	-0.10	0.05	
	literature				
		13	-0.08	0.06	Martin *et al.* (2015)
		11	-0.06	0.04	Tacail *et al.* (2014)
		56	-0.08	0.01	Heuser and Eisenhauer (2008)*

* TIMS analysis

Table S-3 Ca isotope compositions measured in the study relative to ICP-Lyon and SRM915a standards. Conversion between ICP-Lyon and SRM915a standards is given by the relationship: $\delta^{44/42}Ca_{ICP\ Lyon} = \delta^{44/42}Ca_{SRM915a} - 0.52$ (Martin et al. 2015). Error of the $\delta^{44/42}Ca_{SRM915a}$ value is obtained by adding 0.08 ‰ on the error relative to ICP Lyon.

locality	ID	taxon	shape	n	$\delta^{44/42}Ca$ *vs.* ICP Lyon	2 SD	$\delta^{43/42}Ca$ *vs.* ICP Lyon	2 SD	$\delta^{44/42}Ca$ *vs.* SRM915a
Col des Tribes	CT22An	*Ancyrodella*		2	-0.61	0.18	-0.32	0.08	-0.09
	CT22Ag	*Ancyrognathus*		2	-0.59	0.05	-0.28	0.01	-0.07
	CT23Ag	*Ancyrognathus*		3	-0.70	0.09	-0.35	0.01	-0.18
	CT22 (IC1)	*Icriodus*		2	-0.50	0.01	-0.19	0.03	0.02
	CT22 (IC2)	*Icriodus*		2	-0.67	0.32	-0.28	0.10	-0.15
	CT59-7	*Palmatolepis*		2	-0.34	0.12	-0.21	0.00	0.18
	CT37	*Palmatolepis*		2	-0.57	0.10	-0.27	0.07	-0.05
	CT35Pa	*Palmatolepis*		2	-0.60	0.08	-0.31	0.14	-0.08
	CT33	*Palmatolepis*		2	-0.53	0.11	-0.28	0.13	-0.01
	CT30Pa	*Palmatolepis*		2	-0.49	0.01	-0.29	0.02	0.03
	CT23Pa	*Palmatolepis*	Broad	6	-0.61	0.12	-0.30	0.12	-0.09
	CT39Pa	*Palmatolepis*	Broad	2	-0.63	0.07	-0.34	0.00	-0.11
	CT46Pa	*Palmatolepis*	Broad	6	-0.68	0.11	-0.35	0.08	-0.16
	CT51Pa1	*Palmatolepis*	Slender	5	-0.63	0.09	-0.33	0.15	-0.11
	CT51Pa2	*Palmatolepis*	Broad	5	-0.66	0.12	-0.34	0.06	-0.14
	CT54-2Pa	*Palmatolepis*	Broad	6	-0.58	0.12	-0.28	0.11	-0.06
	CT62Pa_1	*Palmatolepis*	Slender	4	-0.53	0.09	-0.26	0.05	-0.01
	CT62Pa_2	*Palmatolepis*	Broad	6	-0.63	0.12	-0.32	0.14	-0.11
	CT69GPa	*Palmatolepis*	Broad	8	-0.53	0.09	-0.28	0.08	-0.01
	CT56Pa	*Palmatolepis*	Broad	3	-0.62	0.01	-0.36	0.07	-0.10
	CT33FRPa	*Palmatolepis*	Broad	3	-0.78	0.13	-0.39	0.14	-0.26
	CT70-2_Pa	*Palmatolepis*	Broad	3	-0.47	0.14	-0.25	0.07	0.05
	CT35Pa0	*Palmatolepis*	Broad	3	-0.84	0.21	-0.48	0.13	-0.32
	CT22Pa	*Palmatolepis*	Broad	3	-0.76	0.10	-0.39	0.09	-0.24
	CT22 (Pa1)	*Palmatolepis*	Broad	2	-0.67	0.18	-0.40	0.09	-0.15
	CT22 (Pa2)	*Palmatolepis*	Broad	2	-0.73	0.15	-0.43	0.01	-0.21
	CT66Pa	*Palmatolepis*	Broad	2	-0.68	0.07	-0.36	0.03	-0.16
	CT66 (Pa5)	*Palmatolepis*	Broad	2	-0.60	0.02	-0.36	0.00	-0.08
	CT66 (Pa6)	*Palmatolepis*	Broad	2	-0.60	0.14	-0.34	0.04	-0.08
	CT66 (Pa7)	*Palmatolepis*	Broad	2	-0.67	0.10	-0.42	0.10	-0.15
	CT30Po	*Polygnathus*		3	-0.54	0.03	-0.29	0.06	-0.02
	CT46Po	*Polygnathus*		3	-0.59	0.06	-0.30	0.03	-0.07
	CT69GPo	*Polygnathus*		4	-0.51	0.08	-0.26	0.10	0.01
	CT39Po	*Polygnathus*		7	-0.61	0.09	-0.33	0.10	-0.09
	CT22Po	*Polygnathus*		2	-0.62	0.03	-0.29	0.05	-0.10
	CT51Po	*Polygnathus*		4	-0.55	0.00	-0.28	0.07	-0.03
	CT22 (Po1)	*Polygnathus*		2	-0.66	0.26	-0.25	0.20	-0.14
	CT22 (Po2)	*Polygnathus*		2	-0.83	0.11	-0.45	0.01	-0.31
	CT22 (Po3)	*Polygnathus*		2	-0.67	0.03	-0.31	0.07	-0.15

Coumiac	CUQ31cAn	*Ancyrodella*		2	-0.54	0.11	-0.29	0.02	-0.02
	CLQ25aAn	*Ancyrodella*		2	-0.59	0.01	-0.25	0.07	-0.07
	CUQ28cAn	*Ancyrodella*		2	-0.62	0.01	-0.32	0.02	-0.10
	CLQ25bAn	*Ancyrodella*		3	-0.71	0.10	-0.37	0.06	-0.19
	CLQ23An	*Ancyrodella*		3	-0.30	0.12	-0.16	0.15	0.22
	CLQ24An	*Ancyrodella*		3	-0.64	0.13	-0.32	0.02	-0.12
	CLQ25aAn	*Ancyrodella*		2	-0.47	0.20	-0.32	0.12	0.05
	CLQ25bAn	*Ancyrodella*		3	-0.60	0.14	-0.31	0.19	-0.08
	CLQ25aAg	*Ancyrognathus*		3	-0.58	0.08	-0.28	0.03	-0.06
	CLQ23bAg	*Ancyrognathus*		2	-0.59	0.04	-0.30	0.02	-0.07
	CLQ25bAg	*Ancyrognathus*		2	-0.77	0.07	-0.40	0.11	-0.25
	CUQ31cAg	*Ancyrognathus*		1	-0.54		-0.29		-0.02
	CUQ28cAg	*Ancyrognathus*		2	-0.49	0.03	-0.24	0.03	0.03
	CLQ23Ag	*Ancyrognathus*		3	-0.39	0.02	-0.14	0.14	0.13
	CLQ24Ag	*Ancyrognathus*		4	-0.60	0.13	-0.33	0.12	-0.08
	CLQ28Ic	*Icriodus*		2	-0.90	0.01	-0.50	0.03	-0.38
	CLQ29aIc	*Icriodus*		2	-0.75	0.11	-0.39	0.01	-0.23
	CLQ33Ic	*Icriodus*		2	-0.86	0.03	-0.48	0.06	-0.34
	CLQ23Pa	*Palmatolepis*		3	-0.72	0.19	-0.38	0.14	-0.20
	CLQ24Pa	*Palmatolepis*		3	-0.74	0.10	-0.39	0.10	-0.22
	CLQ25aPa	*Palmatolepis*		3	-0.78	0.15	-0.41	0.11	-0.26
	CLQ25bPa	*Palmatolepis*		6	-0.58	0.10	-0.31	0.10	-0.06
	CLQ26aPa	*Palmatolepis*		3	-0.75	0.12	-0.38	0.08	-0.23
	CLQ26bPa	*Palmatolepis*		2	-0.63	0.04	-0.33	0.10	-0.11
	CLQ27Pa	*Palmatolepis*		3	-0.70	0.12	-0.36	0.13	-0.18
	CLQ28Pa	*Palmatolepis*		3	-0.78	0.08	-0.39	0.11	-0.26
	CLQ29aPa	*Palmatolepis*		3	-0.81	0.08	-0.43	0.01	-0.29
	CLQ33Pa	*Palmatolepis*		2	-0.69	0.06	-0.40	0.07	-0.17
	CLQ25aPo	*Polygnathus*		3	-0.49	0.05	-0.25	0.02	0.03
	CLQ25bPo	*Polygnathus*		3	-0.56	0.16	-0.29	0.07	-0.04
	CLQ29aPo	*Polygnathus*		3	-0.49	0.11	-0.22	0.08	0.03
	CLQ26bPo	*Polygnathus*		3	-0.78	0.07	-0.43	0.09	-0.26
	CLQ28Po	*Polygnathus*		2	-0.78	0.07	-0.39	0.08	-0.26
M'rirt	M9-1An	*Ancyrodella*		2	-0.62	0.09	-0.32	0.01	-0.10
	M9-2An	*Ancyrodella*		2	-0.59	0.08	-0.29	0.04	-0.07
	M9-1Ag	*Ancyrognathus*		2	-0.47	0.02	-0.21	0.02	0.05
	M9-2Ag	*Ancyrognathus*		2	-0.54	0.19	-0.29	0.06	-0.02
	M9Pa	*Palmatolepis*		2	-0.52	0.05	-0.25	0.05	0.00
Xom Nha	XNAn	*Ancyrodella*		3	-0.64	0.06	-0.33	0.03	-0.12
	XNPa	*Palmatolepis*		2	-0.67	0.14	-0.34	0.09	-0.15
Sprite Ridge	SR1	*Palmatolepis*		2	-0.57	0.10	-0.33	0.08	-0.05
La Serre	LSbrach	brachiopod		3	-0.39	0.07	-0.20	0.03	0.13

Table S-4 Statistical results (*p*-value) of Student's *t*-tests between conodont genera. Under the null hypothesis that there is no difference in the distribution of two groups of $\delta^{44/42}$Ca values, the *p*-value provides the smallest level of significance at which null hypothesis would be rejected. (NS, non significant *p* value; *p = 0.01–0.05; **p = 0.001–0.01; and ***p < 0.001).

	Ancyrodella	***Ancyrognathus***	***Icriodus***	***Palmatolepis***	***Polygnathus***
Ancyrodella		NS 0.849	NS 0.092	NS 0.092	NS 0.327
Ancyrognathus			NS 0.080	NS 0.068	NS 0.253
Icriodus				NS 0.250	NS 0.190
Palmatolepis					NS 0.586
Polygnathus					

Table S-5 Statistical results (correlation coefficient and associated p-value) of Student's t-tests between geochemical proxies used in the study (NS, non significant p value; *p = 0.01–0.05; **p = 0.001–0.01; and ***p < 0.001).

	$\delta^{44/42}$Ca	**δ^{18}O**	**Sr/Ca**	**La/Yb**	**La/Sm**
$\delta^{44/42}$Ca		-0.676, NS 0.066	0.730, NS 0.062	0.518, NS 0.233	0.483, NS 0.273
δ^{18}O			-0.578, NS 0.174	0.048, NS 0.918	0.139, NS 0.767
Sr/Ca				0.139, NS 0.767	0.152, NS 0.745
La/Yb					0.958, *** $<10^{-4}$
La/Sm					

Supplementary Figures

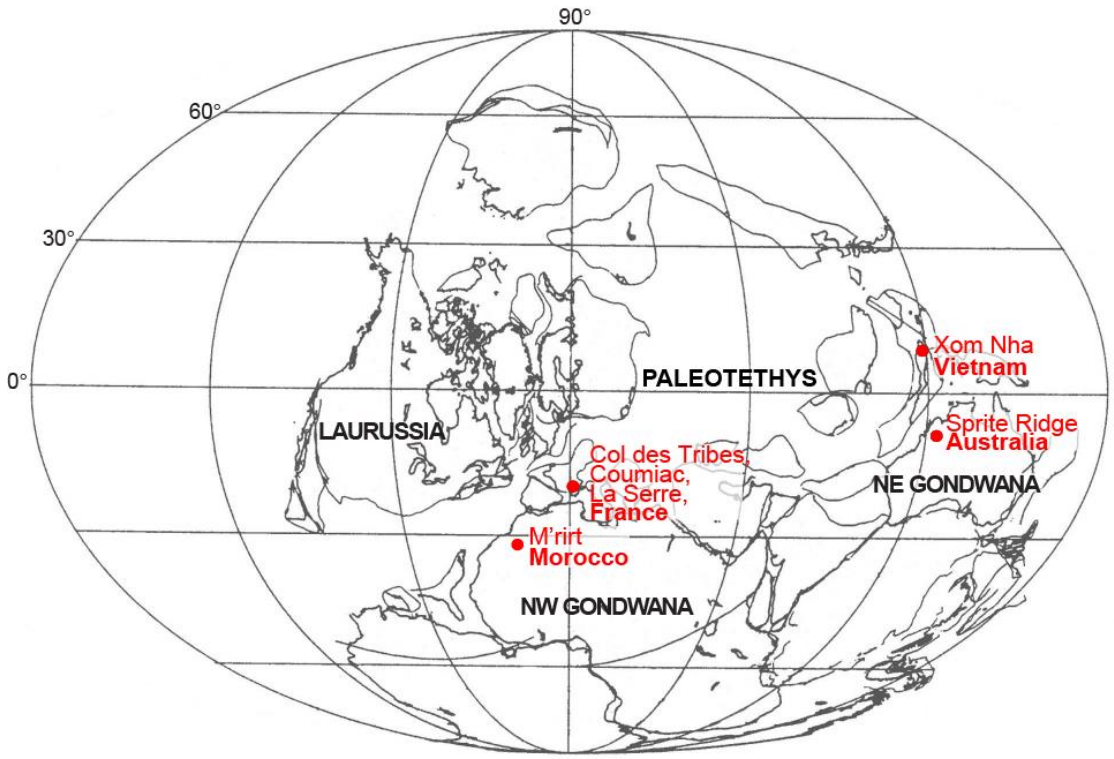

Figure S-1 Localisation of the different sites discussed in the text. Absolute ages are for Col des Tribes, -374 to -360 My; Coumiac, -374 to -371 My; Mrirt and Xom Nha: around -373 My; Sprite Ridge, around 367.5 My. La Serre, -360 My. Ages are from Becker et al. (2012). Conodonts are distributed as following: Col des Tribes, n = 39 (*Palmatolepis*, n=25; *Ancyrodella*, n=1; *Ancyrognathus*, n=2; *Icriodus* n=2; *Polygnathus*, n=9); Coumiac, n = 32 (*Palmatolepis*, n=10; *Ancyrodella*, n=8; *Ancyrognathus*, n=7; *Icriodus* n=2; *Polygnathus*, n=5); M'rirt, n = 5 (*Ancyrodella,* n=2; *Ancyrognathus,* n=2; *Palmatolepis*, n=1); Xhom Nha, n = 2 (*Ancyrodella*, n=1; *Palmatolepis,* n=1); Sprite Ridge, n = 1 (*Palmatolepis*).

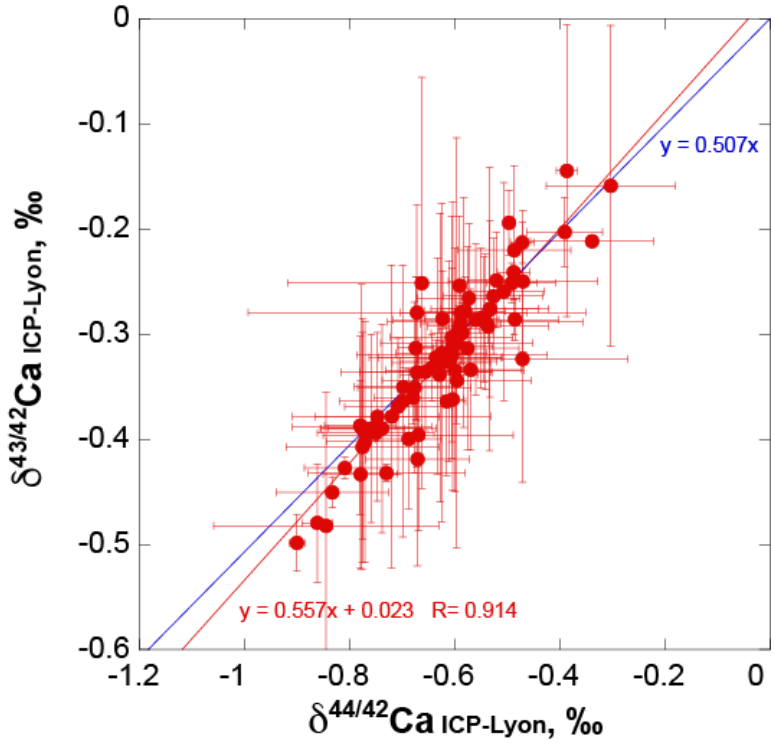

Figure S-2 Three isotopes plot: $\delta^{43/42}$Ca values as a function of the $\delta^{44/42}$Ca values (‰, reference standard ICP Ca-Lyon) for all samples and standards analysed in this study. Ca isotope compositions fall on a line with a y-axis intercept of 0.023 indistinguishable from theoretical 0 ‰ intercept. The slope value of this line is 0.557 (in red) very similar from the 0.507 slope (in blue) predicted by the exponential mass-dependent fractionation law.

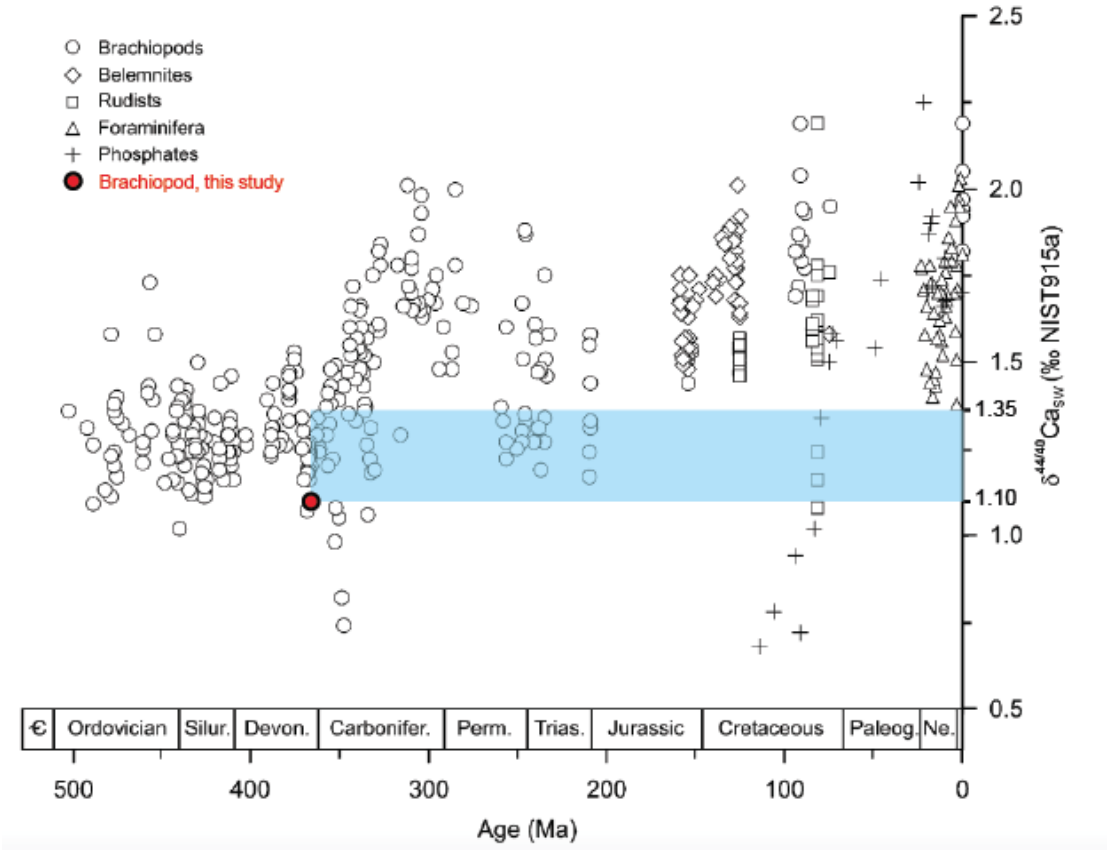

Figure S-3 Value of the $\delta^{44/40}Ca$ of seawater reconstructed from the brachiopod analysed in this study (in red) in the context of the Phanerozoic variations published by Farkaš *et al.* (2007).

Supplementary Information References

Becker, R.T., Gradstein F.M., Hammer O. (2012) The Devonian Period. In: F.M. Gradstein, J.G. Ogg, M.D. Schmitz and G. M. Ogg. (Eds.) *The Geologic Time Scale 2012* Oxford, Elsevier. Volume 2, 559-602.

Brazier, J.-M., Suan, G., Tacail, T., Simon, L., Mattioli, E., Martin, J.E., Balter, V. (2015) Calcium isotope evidence for dramatic increase of continental weathering during the Toarcian Oceanic Anoxic Event (Early Jurassic). *Earth and Planetary Science Letters* 411, 164-176.

Farkaš, J., Böhm, F., Wallmann, K., Blenkinsop, J., Eisenhauer, A., van Geldern, R., Munnecke, A., Voigt, S., Veizer, J. (2007) Calcium isotope record of Phanerozoic oceans: implications for chemical evolution of seawater and its causative mechanisms. *Geochimica Cosmochimica Acta* 71, 5117-5134.

Feist, R., Becker, R.T. (1997) Discovery of Famennian trilobites in Australia (Late Devonian, Canning Basin, NW Australia). *Geobios* 20, 231-242.

Flajs, G., Feist, R. (1988) Index conodonts, trilobites and environment of the Devonian/Carboniferous boundary beds at La Serre (Montagne Noire, France). Devonian-Carboniferous boundary — Results of recent studies. *Courier Forschungsinstitut Senckenberg* 100, 53-107.

Girard, C., Feist, R. (1997) Eustatic trends in conodont diversity across the Frasnian/Famennian boundary in the stratotype area, Montagne Noire, France. *Lethaia* 29, 329-337.

Girard, C., Klapper, G., Feist, R. (2005) Subdivision of the terminal Frasnian linguiformis conodont Zone, revision of the correlative interval of Montagne Noire Zone 13, and discussion of stratigraphically significant associated trilobites. In: Over, D.J., Morrow, J.R., Wignall, P.B. (Eds.) *Understanding Late Devonian and Permian-Triassic Biotic and Climatic Events: Towards an integrated approach.* Developments in Palaeontology and Stratigraphy Series, pp. 181-198.

Girard, C., Phuong, T.H., Savage, N.M., Renaud S. (2010) Temporal dynamics of the geographic differentiation of Late Devonian *Palmatolepis* assemblages in the Prototethys. *Acta Palaeontologica Polonica* 55, 675-687.

Girard, C., Cornée, J.-J., Corradini, C., Fravalo, A., Feist, R. (2014) Palaeoenvironmental changes at Col des Tribes (Montagne Noire, France), a reference section for the Famennian of north Gondwana-related areas. *Geological Magazine* 151, 864-884.

Joachimski, M.M., Buggisch, W., (1993) Anoxic events in the late Frasnian-Causes of the Frasnian-Famennian faunal crisis?: *Geology*, 21, 675-678.

Heuser, A., Eisenhauer, A. (2008) The Calcium Isotope Composition ($\delta^{44/40}$Ca) of NIST SRM 915b and NIST SRM 1486. *Geostandards Geoanalytical Research* 32, 311–315.

Heuser, A., Tütken, T., Gussone, N., Galer, S.J.G. (2011) Calcium isotopes in fossil bones and teeth — Diagenetic versus biogenic origin. *Geochimica et Cosmochimica Acta* 75, 3419–3433.

Lazreq, N. (1999) Biostratigraphie des conodontes du Givétien au Famennien du Maroc central - Biofaciès et événement Kellwasser. *Courier Forschungsinstitut Senckenberg* 214, 1-111.

Le Houedec, S., Girard, C., Balter, V. (2013) Conodont Sr/Ca and δ^{18}O record seawater changes at the Frasnian-Famennian boundary. *Palaeogeography, Palaeoclimatology, Palaeoecology* 376, 114-121.

Martin, J. E., Tacail, T., Adnet, S., Girard, C., Balter, V. (2015) Calcium isotopes reveal the trophic position of extant and fossil elasmobranchs: *Chemical Geology* 415, 118-125.

Martin, J. E., Tacail, T., and Balter, V. (2017) Non-traditional isotope perspectives in vertebrate palaeobiology. *Palaeontology* 60, 485-502.

Phuong, T.H. (1998) Upper Devonian Conodont Biostratigraphy in Viêt Nam. *Journal of Geology Series B*, 11-12, 76-84.

Pruss, S.B., Blättler, C.L., Macdonald, F.A., Higgins, J.A. (2018) Calcium isotope evidence that the earliest metazoan biomineralizers formed aragonite shells. *Geology* 46, 763-766.

Reynard, B., Balter, V. (2014) Trace elements and their isotopes in bones and teeth: diet, environments, diagenesis, and dating of archeological and paleontological samples. *Palaeogeography, Palaeoclimatology, Palaeoecology* 416, 4-16.

Tacail, T., Albalat, E., Télouk, P., Balter, V. (2014) A simplified protocol for the measurement of Ca isotopes in biological samples. *Journal of Analytical Atomic Spectrometry* 29, 529-535.